Electronic Supplementary Information

Experimental Section

Materials: Cu foam was purchased from Suzhou Taili New Energy Co., Ltd. Nafion (5 wt%) solution, $RuCl_3 \cdot 3H_2O$ and TCNQ were purchased from Sigma-Aldrich Chemical Reagent Co., Ltd. Hydrochloric acid (HCl), ethanol and acetonitrile were purchased from Aladdin Ltd. (Shanghai, China). All reagents were used as received. The water used throughout all experiments was purified through a Millipore system.

Preparation of Cu(TCNQ) NA/CF and Cu-N-C NA/CF: Cu foam was washed with ethanol and water several times, and then submitted to sonication with concentrated HCl at 30 °C for 15 min to remove the surface impurities. A 3 cm × 1 cm ×0.2 cm strip of Cu foam was placed in 6 mL of 2 mM TCNQ/acetonitrile solution for 7 h. The surface of Cu foam was observed to turn dark purple, indicating that Cu(TCNQ) NA/CF was synthesized through a spontaneous crystallization process. Then the Cu(TCNQ) NA/CF was washed three times with deionized water and dried under N_2 gas. Subsequently, the sample was heated at temperatures of 600 °C for 2 h in Ar atmosphere, and then cooled to ambient temperature under Ar atmosphere to make Cu-N-C NA/CF.

Synthesis of RuO_2: RuO_2 was prepared according to the previous report.[1] Briefly, 2.61 g of $RuCl_3 \cdot 3H_2O$ and 1.0 mL NaOH (1.0 M) were added into 100 mL distilled water and stirred for 45 min at 100 °C. Then the solution was centrifuged for 10 minutes and filtered. The precipitate was collected and washed with water several times. Finally, the product was dried at 80 °C overnight and then annealed at 300 °C in air for 3 h. 20 mg RuO_2 and 10 μL 5 wt% Nafion solution were dispersed in 990 μL water/ethanol (V:V = 1:1) by 30 min sonication to form a catalyst ink. Then 44.25 μL catalyst ink was loaded on Cu foam with a loading mass of ~ 1.77 mg cm^{-2}.

Characterizations: The X-ray diffraction (XRD) patterns were obtained from a LabX XRD-6100 X-ray diffractometer with Cu Kα radiation (40 kV, 30 mA) of wavelength 0.154 nm (SHIMADZU, Japan). Scanning electron microscope (SEM) measurements were recorded on a XL30 ESEM FEG scanning electron microscope at an accelerating voltage of 20 kV. Transmission electron microscopy (TEM) images were made on a HITACHI H-8100 electron microscopy (Hitachi, Tokyo, Japan) with an accelerating voltage of 200 kV. X-ray photoelectron spectroscopy (XPS) was conducted on an ESCALABMK II X-ray photoelectron spectrometer using Mg as the exciting source.

Electrochemical measurements: Electrochemical measurements were performed with a CHI 660E electrochemical analyzer (CH Instruments, Inc., Shanghai) in a standard three-electrode system using a Cu-N-C NA/CF as the working electrode, a graphite rod as the counter electrode and a Hg/HgO as the reference electrode. The potentials reported in this work were calibrated to RHE, using the following equation: E (RHE) = E (Hg/HgO) + (0.098 + 0.059 pH) V. Polarization curves were obtained using linear sweep voltammetry with a scan rate of 5 mV s^{-1}. Pressure data during electrolysis were recorded using a CEM DT-8890 Differential Air Pressure Gauge Manometer Data Logger Meter Tester with a sampling interval of 1 point per second. All experiments were carried out at room temperature (~ 25 °C).

Diameter calculation: The diameter of Cu nanoparticles are calculated by the Scherrer equation:

$$D = K\lambda/(\beta\cos\theta)$$

Where K is the Scherrer constant (K = 0.89); λ is the wave length of diffracted wave (λ = 0.154 nm); θ is the angle of diffraction; β is the width of half height (FWHM) which should be applied in radian measure.

In the diameter calculation, the β is obtained from the Jade software analysis with the value of 0.842 of the two main peaks of Cu in Figure S1. The calculated D is the average height of the nanocrystal which is grown perpendicular to the orientation of the lattice plane.

Turnover frequencies (TOF) calculation: The TOF for each active site was calculated by the equation:

$$TOF = JA/4Fm$$

Where J is current density (A cm^{-2}) at defined overpotential of the electrochemical measurement in 1.0 M KOH; A is the geometric area of the testing electrode; 4

indicates the mole of electrons consumed for evolving one mole O_2; F is the Faradic constant (96485 C mol^{-1}); m is the number of active sites (mol), which can be extracted from the linear relationship between the oxidation peak currents and scan rates by the equation:

$$\text{slope} = n^2F^2A\Gamma_0/4RT$$

Where n is the numbers of electron transferred; Γ_0 is the surface concentration of active sites (mol cm^{-2}); R and T are the ideal gas constant and the absolute temperature, respectively.

Determination of Faradaic efficiency (FE)*:* The oxygen generated at anode was confirmed by gas chromatography (GC) analysis and measured quantitatively by using a calibrated pressure sensor to monitor the pressure change in the anode compartment of a H-type electrolytic cell. The FE was calculated by comparing the amount of experimentally measured oxygen generated by potentiostatic anodic electrolysis with theoretically calculated oxygen (assuming 100% FE). GC analysis was carried out on GC-2014C (Shimadzu Co.) with thermal conductivity detector and nitrogen carrier gas. Pressure data during electrolysis were recorded using a CEM DT-8890 Differential Air Pressure Gauge Manometer Data Logger Meter Tester with a sampling interval of one point per second.

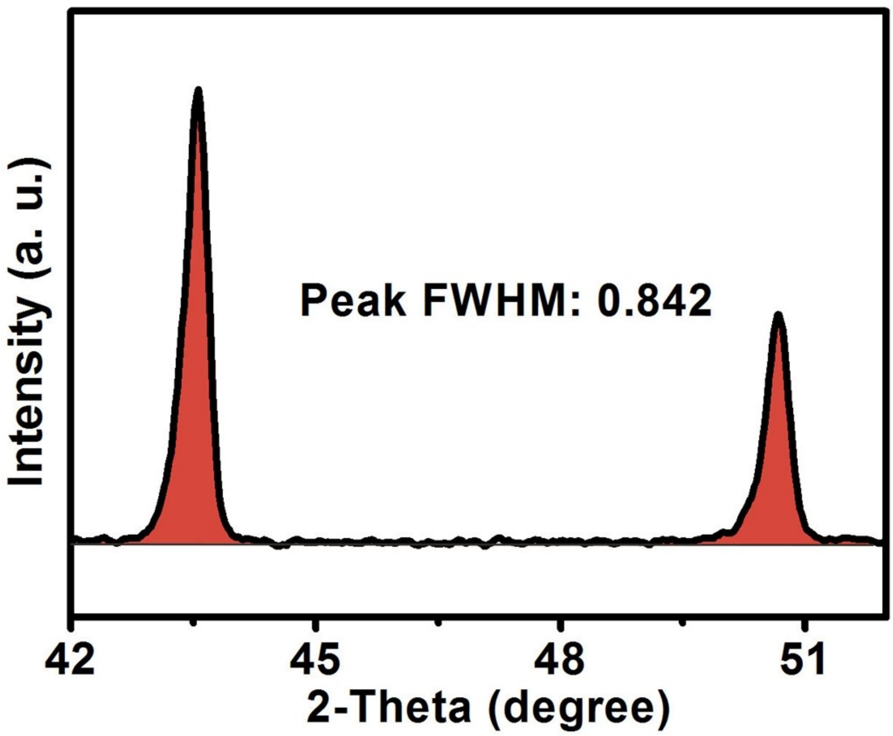

Fig. S1. XRD pattern of Cu-N-C in the diffraction angle range of 42-52°.

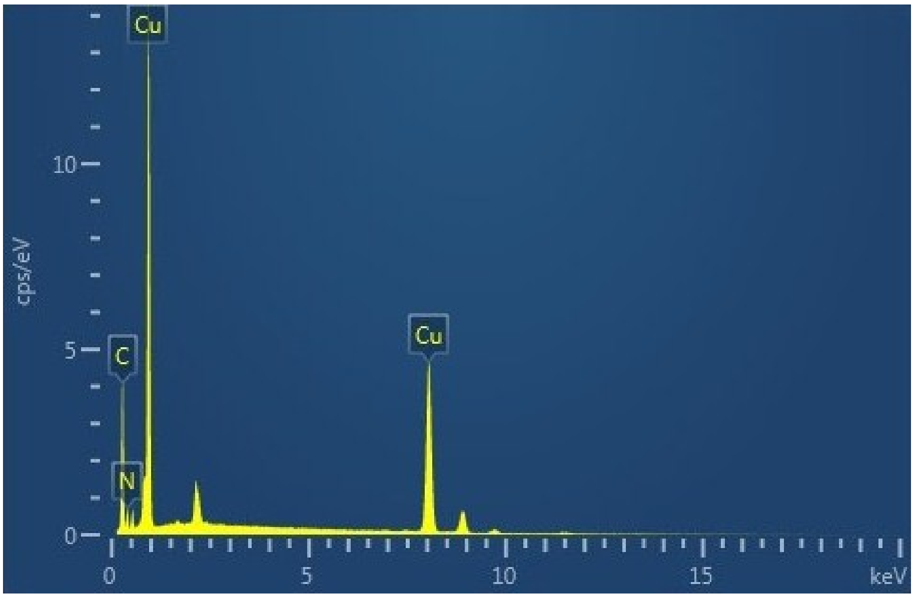

Fig. S2. EDX spectrum of Cu-N-C NA/CF.

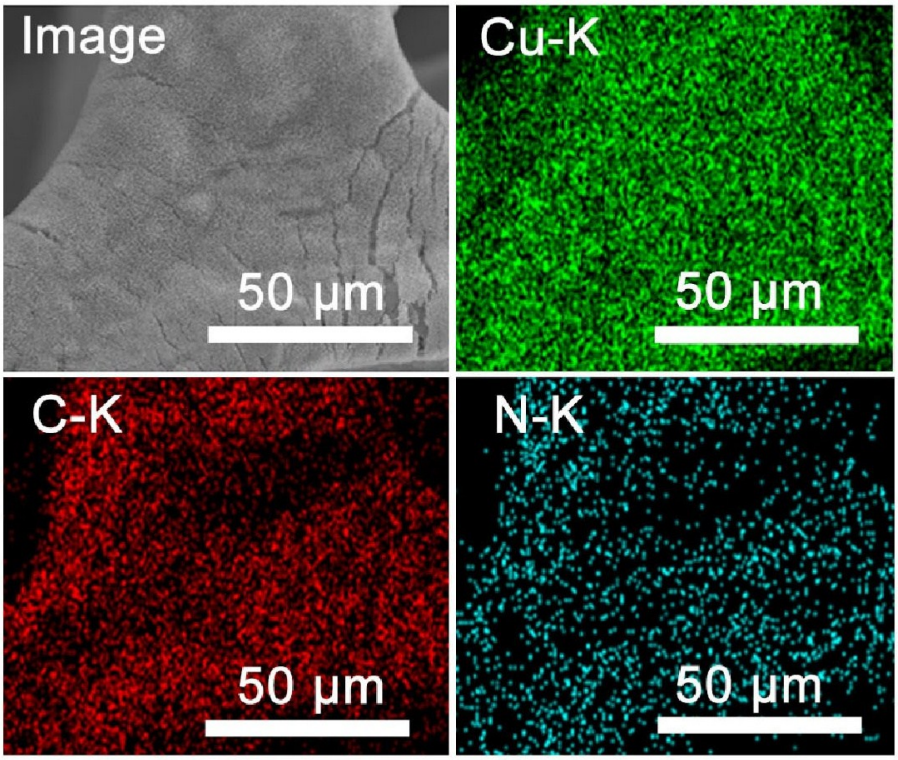

Fig. S3. EDX elemental mapping images of Cu, C, and N for Cu-N-C NA/CF.

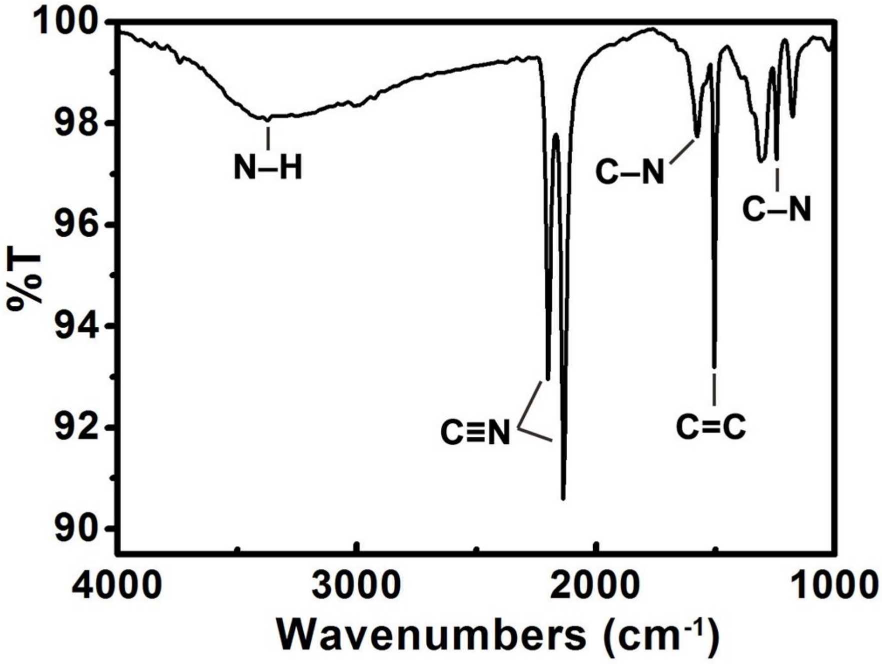

Fig. S4. FT-IR spectrum of Cu-N-C.

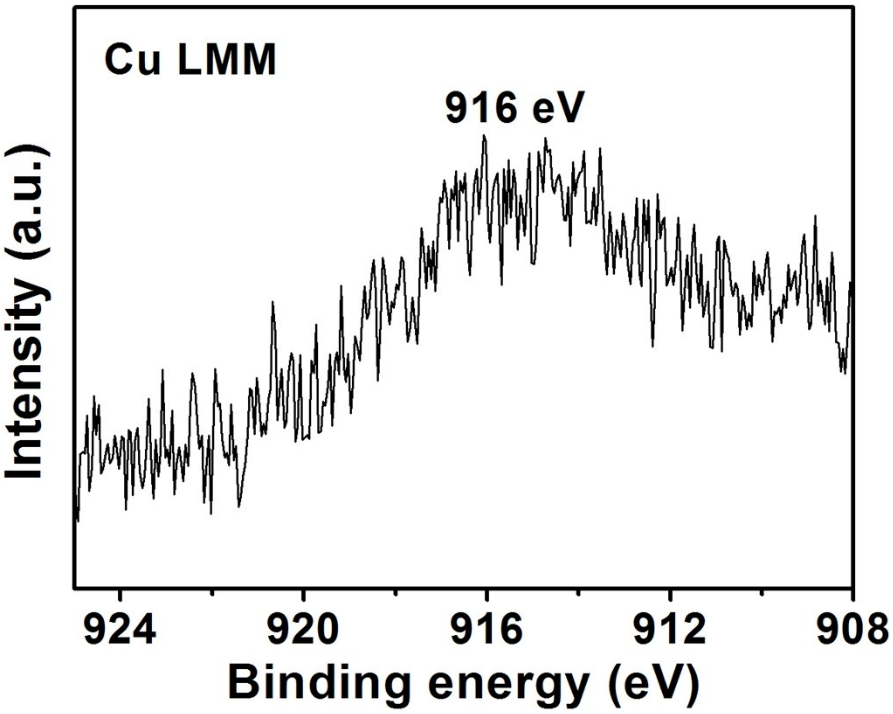

Fig. S5. Cu LMM of Cu-N-C.

Table S1. Comparison of catalytic performance for Cu-N-C NA/CF with other non-noble-metal OER catalysts in alkaline media.

Catalyst	***J*** **(mA cm^{-2})**	***η*** **(mV)**	**Electrolyte**	**Ref.**
Cu-N-C NW/CF	10	243	1.0 M KOH	This work
	50	352		
	20	405	0.1 M KOH	
dendritic copper oxide ($Cu/Cu_2O/CuO$)	50	~425	1.0 M NaOH	2
nanostructured Cu oxide	5	550	1.0 M NaOH	2
$Cu/Cu(OH)_2$-CuO nanorods	10	417	0.1 M KOH	3
Cu oxide film	10	430	1.0 M KOH	4
heterogeneous CuO	10	430	1.0 M KOH	4
CuO nanowires	10	530	0.1 M NaOH	5
Cu_2O nanowires	10	590	0.1 M NaOH	5)
CuO_x nanowires	10	630	0.1 M NaOH	5)
2D CuO nanosheet bundles	10	350	1.0 M KOH	6
Cu_2O/C	10	330	1.0 M KOH	7
Cu_2O/Cu	1	~ 450	0.1 M KOH	8
CuS NCs	10	454	0.1 M KOH	9
CoP nanoparticles	10	320	1.0 M KOH	10
Ni_2P nanoparticles	10	500	1.0 M KOH	11
FeCoW (on glassy carbon)	10	223	1.0 M KOH	12
Ni_2P/Ni foam	10	290	1.0 M KOH	13
NiS nanosheet	10	297	1.0 M KOH	14
NiFe-LDH/Ni foam	10	240	1.0 M KOH	15
Co_3O_4/MNTs	25	~373	1.0 M KOH	16
NiO	10	364	1.0 M KOH	17
N-CG-CoO hybrid	25	~385	1.0 M KOH	18
Co_3O_4@C-MWCNTs	10	320	1.0 M KOH	19

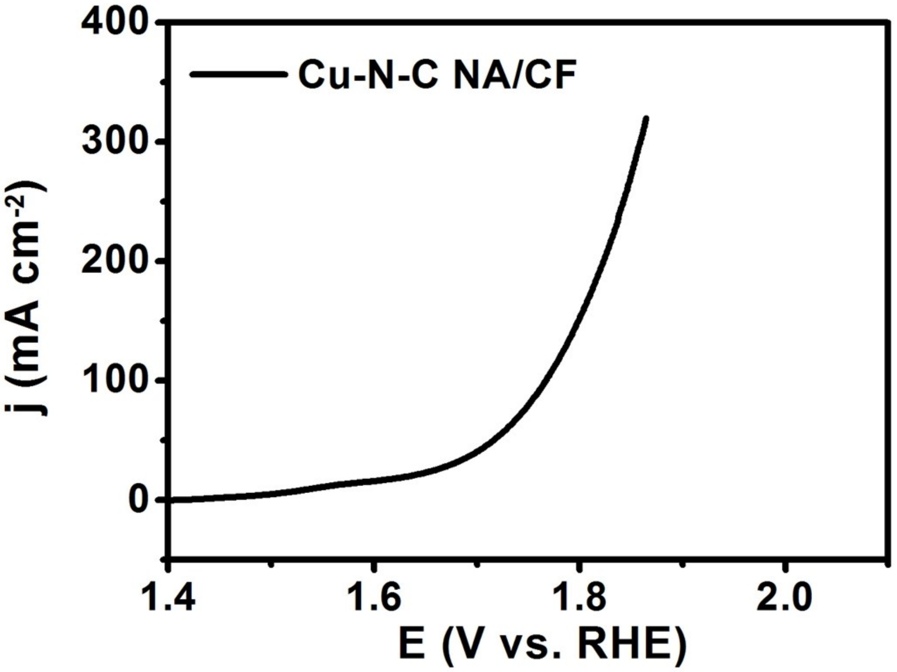

Fig. S6. LSV curve for OER of Cu-N-C NA/CF in 0.1 M KOH.

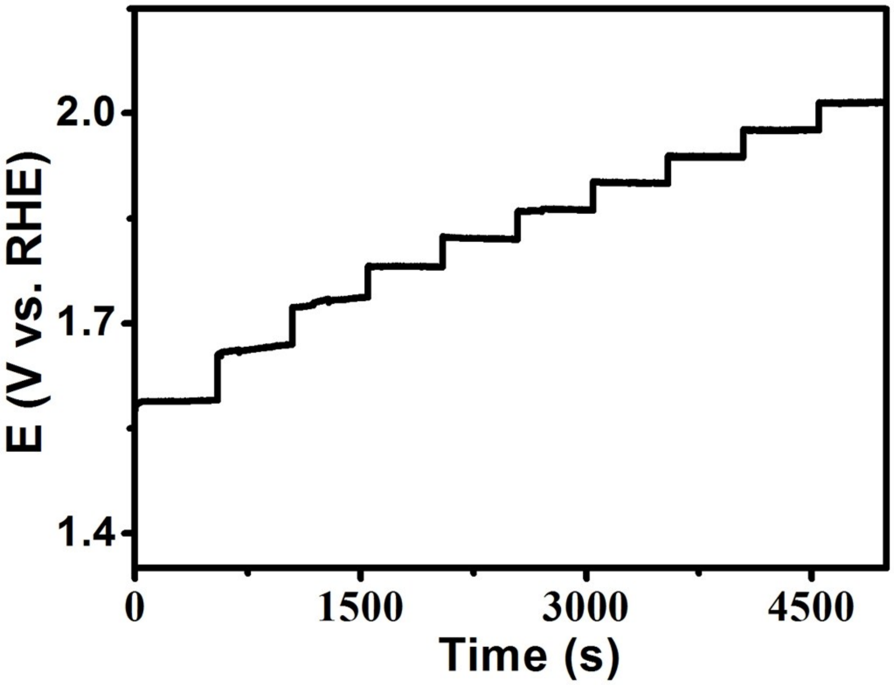

Fig. S7. Multi-current process of Cu-N-C NA/CF. The current density started at 10 mA cm^{-2} and ended at 100 mA cm^{-2}, with an increment of 10 mA cm^{-2} per 500 s without iR correction.

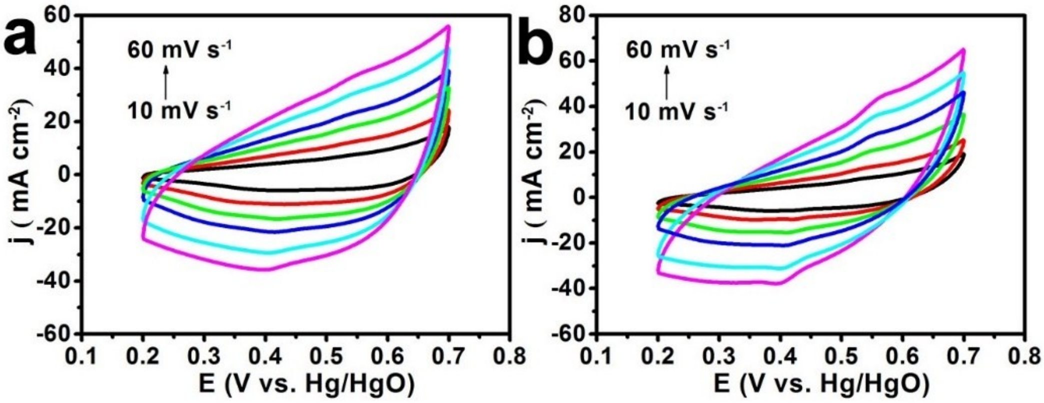

Fig. S8. CVs in the region of 0.2 V to 0.7 V vs. Hg/HgO for (a) Cu(TCNQ) NA/CF and (b) Cu-N-C NA/CF.

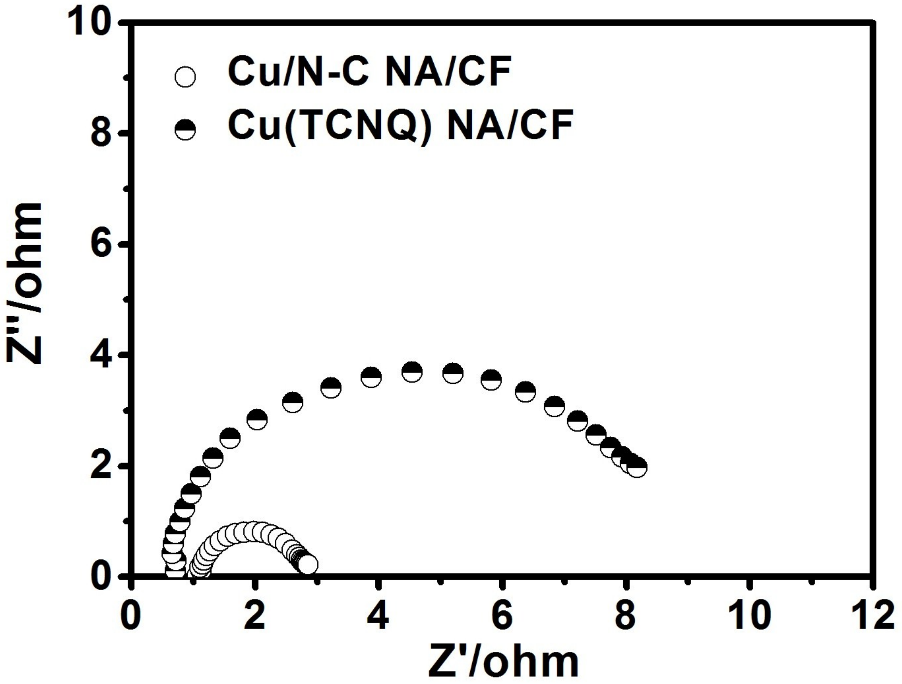

Fig. S9. EIS data of Cu(TCNQ) NA/CF and Cu-N-C NA/CF measured in 1.0 M KOH.

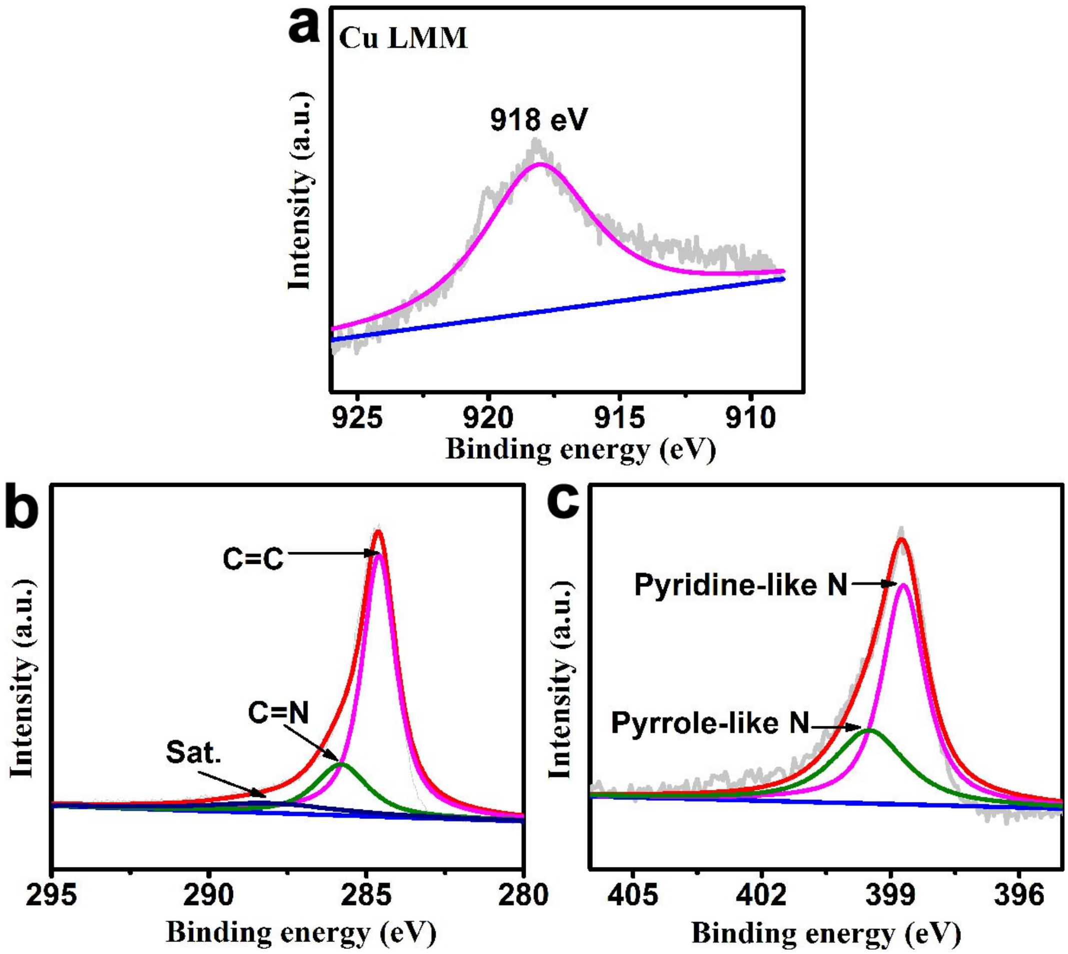

Fig. S10. XPS spectra of Cu-N-C after OER electrolysis in the (a) Cu LMM, (b) C 1s, and (c) N 1s regions.

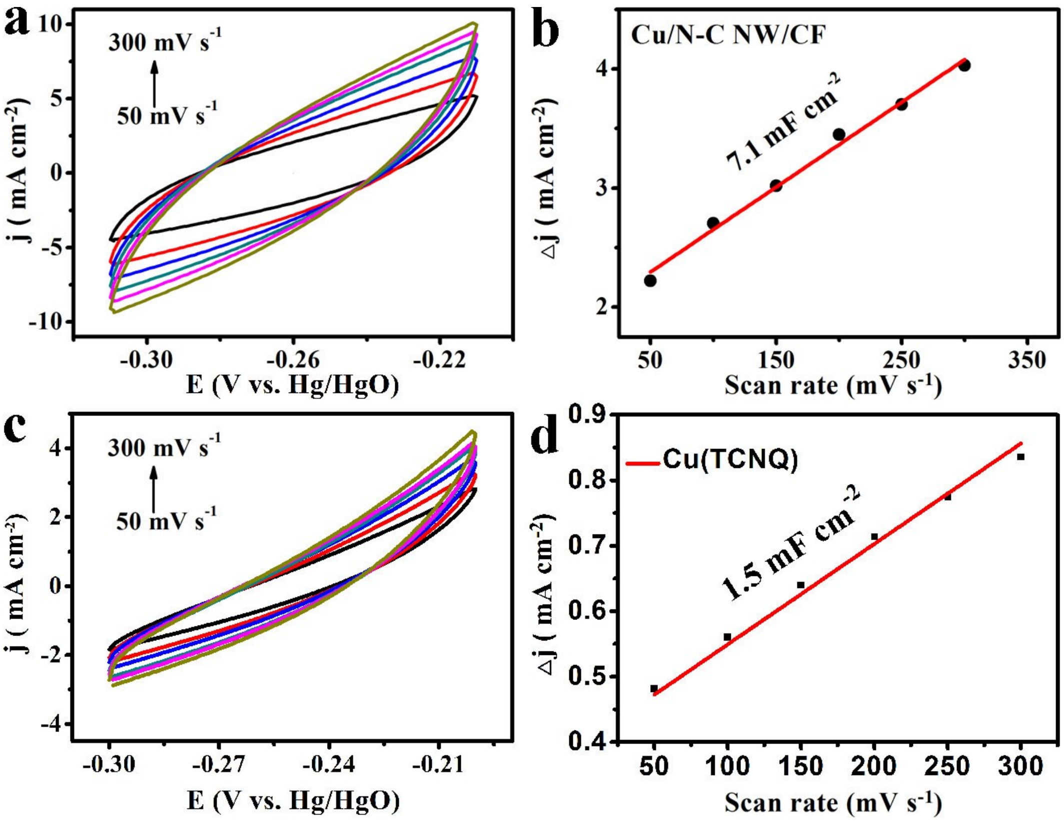

Fig. S11. Cyclic voltammograms of (a) Cu-N-C/NF (c) Cu(TCNQ)/NF in the non-faradaic capacitance current range at scan rates of 50, 100, 150, 200, 250 and 300 mV s^{-1}. (b) and (d) the capacitive currents at certain potential as a function of scan rate for Cu-N-C/NF and Cu(TCNQ)/NF.

References

1 J. Cruz, V. Baglio, S. Siracusano, V. Antonucci, A. Aricò, R. Ornelas, L. Ortiz-Frade, G. Osorio-Monreal, S. Durón-Torres and L. Arriaga, *Int. J. Electrochem. Sci.,* 2011, **6**, 6607–6619.

2 T. N. Huan, G. Rousse, S. Zanna, I. T. Lucas, X. Xu, N. Menguy, V. Mougel and M. Fontecave, *Angew. Chem., Int. Ed.,* 2017, **56**, 4792–4796.

3 N. Cheng, Y. Xue, Q. Liu, J. Tian, L. Zhang, A. M. Asiri and X. Sun, *Electrochim. Acta,* 2015, **163**, 102–106.

4 X. Liu, S. Cui, Z. Sun, Y. Ren, X. Zhang and P. J. Du, *Phys. Chem. C,* 2016, **120**, 831–840.

5 C.-C. Hou, W.-F. Fu and Y. Chen, *ChemSusChem,* 2016, **9**, 2069–2073.

6 S. M. Pawar, B. S. Pawar, B. Hou, J. Kim, A. T. A. Ahmed, H. S. Chavan, Y. Jo, S. Cho, A. I. Inamdar, J. L. Gunjakar, H. Kim, S. Cha and H. Im, *J. Mater. Chem. A,* 2017, **5,** 12747–12751.

7 H. Zhang, Z. Zhang, N. Li, W. Yan and Z. Zhu, *J. Catal.,* 2017, **352**, 239–245.

8 Y. Deng, A. D. Handoko, Y. Du, S. Xi and B. S. Yeo, *ACS Catal.,* 2016, **6**, 2473–2481.

9 L. An, Y. Li, M. Luo, J. Yin, Y.-Q. Zhao, C. Xu, F. Cheng, Y. Yang, P. Xi and S. Guo, *Adv. Funct. Mater.,* 2017, DOI: 10.1002/adfm.201703779.

10 J. F. Chang, Y. Xiao, M. L. Xiao, J. J. Ge, C. P. Liu and W. Xing, *ACS Catal.,* 2015, **5**, 6874–6878.

11 A. Han, H. Chen, Z. Sun, J. Xu and P. Du, *Chem. Commun.,* 2015, **51**, 11626–11629.

12 B. Zhang, X. L. Zheng, O. Voznyy, R. Comin, M. Bajdich, M. Garcia-Melchor, L. L. Han, J. X. Xu, M. Liu, L. R. Zheng, F. P. G. de Arquer, C. T. Dinh, F. J. Fan, M. J. Yuan, E. Yassitepe, N. Chen, T. Regier, P. F. Liu, Y. H. Li, P. De Luna, A. Janmohamed, H. L. L. Xin, H. G. Yang, A. Vojvodic and E. H. Sargent, *Science,* 2016, **352**, 333–337.

13 L. A. Stern, L. Feng, F. Song and X. Hu, *Energy Environ. Sci.,* 2015, **8**, 2347–2351.

14 J. S. Chen, J. Ren, M. Shalom, T. Fellinger and M. Antonietti, *ACS Appl. Mater. Interfaces,* 2016, **8**, 5509–5516.

15 J. Luo, J.-H. Im, M. T. Mayer, M. Schreier, M. K. Nazeeruddin, N.-G. Park, S. D. Tilley, H. J. Fan and M. Grätzel, *Science,* 2014, **345**, 1593–1596.

16 H. Wang, S. Zhu, Y. Liang, X. Han and B. Zhang, *Angew. Chem., Int. Ed.,* 2016, **55**, 9055–9059.

17 L. A. Stern, L. Feng, F. Song and X. Hu, *Energy Environ. Sci.,* 2015, **8**, 2347–2351.

18 S. Mao, Z. Wen, T. Huang, Y. Hou and J. Chen, *Energy Environ. Sci.,* 2014, **7,** 609–616.

19 X. Li, Y. Fang, X. Lin, M. Tian, X. An, Y. Fu, R. Li, J. Jin and J. Ma, *J. Mater. Chem. A,* 2015, **3**, 17392–17402.